

## Solving the dual-phase lag bioheat transfer equation by the generalized finite difference method

L. TURCHAN

*Institute of Computational Mechanics and Engineering  
Silesian University of Technology  
Konarskiego 18A  
44-100 Gliwice, Poland  
e-mail: lukasz.turchan@polsl.pl*

THE MODELING OF BIOHEAT TRANSFER PROCESS described by the dual-phase lag equation is considered. The basic equation is supplemented by the appropriate boundary-initial conditions. In the central part of the cylindrical domain the heated sub-domain is located. In this region the additional component determining the capacity of an internal heat source is taken into account. At the stage of numerical computations the generalized finite difference method (GFDM) is used. The GFDM nodes distribution is generated in a random way (with some limitations). The examples of computations for different nodes distribution and comparison with the classical finite difference method are presented. In the final part of the paper the conclusions are formulated.

**Key words:** bioheat transfer, dual-phase lag model, generalized finite difference method.

Copyright © 2017 by IPPT PAN

### 1. Introduction

THE SUBJECT OF THE PAPER IS CONNECTED WITH the numerical modeling of thermal processes proceeding in the domain of the soft tissues. For many years the base of these processes description was the Pennes equation [1, 2]. It is the typical heat diffusion parabolic equation supplemented by additional terms (the source functions) connected with the blood perfusion and metabolism. The mathematical form of the perfusion heat source results from the assumption that soft tissue is supplied by a big number of capillary blood vessels uniformly distributed in the tissue domain. The metabolic heat source is assumed as a constant value or the temperature-dependent function [3].

To take into account the finite velocity of a thermal wave propagation the so-called relaxation time was introduced by CATTANEO [4] and the energy equation (a hyperbolic PDE) is known as the Cattaneo–Vernotte equation. Because of

the specific inner structure of tissue which causes the lag effect of heat flux with respect to the temperature gradient this equation is also applied in the case of bio-heat transfer [5, 6]. For example, in the paper [5] the relaxation time for processed meat is estimated to be of the order of 2 seconds. In literature, the other values of this parameter can be also found (e.g. [6]).

Recently to describe the heat transfer in the soft tissue domain the dual-phase lag equation (DPLE) has often been used. The DPL model describes a macroscopic temperature, at the same time an inner microscopic tissue structure is taken into account by an introduction of two delay times to the energy equation (e.g. [7, 8]). So, the DPLE contains both the relaxation time  $\tau_q$  and thermalization time  $\tau_T$ . In the equation discussed the second derivative of temperature with respect to time and also the mixed derivative both in time and space appear.

In this paper the presented problem of artificial hyperthermia modeling can be understood as a medical treatment in which the local tissue temperature is raised to 41–46°C. Problems of the thermal processes proceeding in the domain of heated living tissue were analyzed by LIU [9]. Next in 2009, LIU and CHEN [10] used the DPL equation for the hyperthermia treatment modeling. The similar problems are discussed in the papers [11–13]. The authors consider the thermal damage of the biological tissues due to the laser irradiation.

At the stage of computations the different methods of the PDE numerical solutions have been applied. The majority of them based on the classic variant of the finite difference method (FDM) for hyperbolic equations, e.g. [14–17], or its modifications [18, 19]. Quite often the control volume method is also used [12, 13, 20]. One should also mention the use of the finite element method [11] or the boundary element method [21–23].

In this paper the application of the generalized finite difference method (GFDM) is discussed. It is said that the GFDM constitutes, in a certain degree, the bridge between the classical FDM and FEM. It results from the possibility of practically optional discretization of the domain considered (the similar advantages has a version of the control volume method presented in [20]). One of the first publications concerning the GFDM was the paper presented by ORKISZ and LISZKA [24]. The method has been used for the elliptical PDE. The similar topics have been developed in the papers [25, 26]. The GFDM for the parabolic PDE has been used by MOCHNACKI and PAWLAK [27]. In the paper the stability condition for GFDM explicit scheme has also been formulated. In turn, in the paper [28] GFDM was applied for numerical modeling of a solidification process.

In this paper the GFDM is proposed to solve the DPL model describing the bioheat transfer process in an axisymmetrical domain.

According to the author's knowledge the method so far has not been used for this type of thermal diffusion problems.

### 2. Governing equation

The domain of healthy tissue  $\Omega_1$  and centrally located sub-domain of the tumor  $\Omega_2$ , as shown in Fig. 1, is considered. Under the assumption that thermal properties of the healthy tissue and tumor region are the same, only one DPL equation describing the temperature field in the domain  $\Omega_1 \cup \Omega_2$  is considered [13]:

$$(2.1) \quad C \left[ \frac{\partial T(r, z, t)}{\partial t} + \tau_q \frac{\partial^2 T(r, z, t)}{\partial t^2} \right] = \lambda \nabla^2 T(r, z, t) + \lambda \tau_T \frac{\partial \nabla^2 T(r, z, t)}{\partial t} + Q(r, z, t) + \tau_q \frac{\partial Q(r, z, t)}{\partial t},$$

where  $(r, z)$  [m] are the spatial coordinates,  $t$  [s] is the time,  $T$  [°C] is the temperature of tissue,  $C$  [J/(m<sup>3</sup>·K)] is the volumetric specific heat of tissue,  $\lambda$  [W/(m·K)] is the thermal conductivity of tissue, while  $\tau_q$  [s] is a relaxation time and  $\tau_T$  [s] is the thermalization time.

The source function  $Q(r, z, t)$  [W/m<sup>3</sup>] in Eq. (2.1) consists of three components, first one connected with the blood perfusion, next one connected with metabolism  $Q_m$  and last one is the source function  $Q_e$  describing the artificial heating of tissue

$$(2.2) \quad Q(r, z, t) = Gc_b[T_b - T(r, z, t)] + Q_m(r, z, t) + Q_e(r, z, t)$$

where  $G$  [kg/(m<sup>3</sup>·s)] is the blood perfusion rate,  $c_b$  [J/(kg·K)] is the specific heat of blood,  $T_b$  [°C] is the arterial blood temperature,  $Q_m(r, z, t)$  is a metabolic

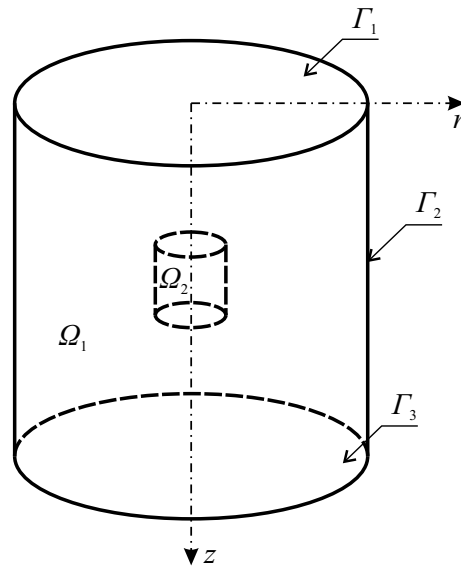


FIG. 1. The considered domain ( $\Omega_1$ ) with a heating zone ( $\Omega_2$ ).

heat source. The function  $Q_e(r, z, t)$  is defined as follows:

$$(2.3) \quad (r, z) \in \Omega_2 : \quad Q_e(r, z, t) = \begin{cases} Q_0, & t \leq t_{ex}, \\ 0, & t > t_{ex}, \end{cases}$$

where  $Q_0$  is a constant value and  $t_{ex}$  is the exposure time. For  $(r, z) \in \Omega_1 : Q_e(r, z, t) = 0$ , of course.

The Eq. (2.1) is supplemented by the no-flux boundary condition  $q(r, z, t) = 0$  and initial conditions:

$$(2.4) \quad t = 0 : \quad T(r, z, 0) = T_p, \quad \frac{\partial T(r, z, 0)}{\partial t} = w,$$

where  $T_p$  is the initial temperature and  $w$  is the initial heating rate.

Taking into account the form of the source function (2.2) and assuming that  $Q_m$  is a constant value, the equation (2.1) can be written as follows

$$(2.5) \quad (C + Gc_b\tau_q) \frac{\partial T(r, z, t)}{\partial t} + C\tau_q \frac{\partial^2 T(r, z, t)}{\partial t^2} \\ = \lambda \left[ \nabla^2 T(r, z, t) + \tau_T \frac{\partial \nabla^2 T(r, z, t)}{\partial t} \right] + Gc_b[T_b - T(r, z, t)] + Q_m + Q_e(r, z, t).$$

The Eq. (2.5) supplemented by boundary and initial conditions is solved using the generalized finite difference method presented in the next section.

### 3. Method of solution

To solve the formulated problem, an explicit scheme of the generalized finite difference method has been used. The time discretisation, with the constant time step  $\Delta t$ , is introduced and the temperature at the node  $i$  is denoted as  $T_i^f = T(r_i, z_i, f\Delta t)$ . So, for time  $t^f = f\Delta t$  ( $f \geq 2$ ) the following approximate form of equation (2.5) is proposed

$$(3.1) \quad (C + Gc_b\tau_q) \frac{T_i^f - T_i^{f-1}}{\Delta t} + C\tau_q \frac{T_i^f - 2T_i^{f-1} + T_i^{f-2}}{(\Delta t)^2} \\ = \lambda \left[ (\nabla^2 T)_i^{f-1} + \tau_T \frac{(\nabla^2 T)_i^{f-1} - (\nabla^2 T)_i^{f-2}}{\Delta t} \right] + Gc_b(T_b - T_i^{f-1}) + Q_m + Q_{e_i}^{f-1},$$

where

$$(3.2) \quad (\nabla^2 T)_i^s = \left[ \frac{1}{r} \frac{\partial}{\partial r} \left( r \frac{\partial T}{\partial r} \right) + \frac{\partial^2 T}{\partial z^2} \right]_i^s \\ = \left( \frac{1}{r} \frac{\partial T}{\partial r} + \frac{\partial^2 T}{\partial r^2} + \frac{\partial^2 T}{\partial z^2} \right)_i^s = \frac{1}{r} T_r^s + T_{rr}^s + T_{zz}^s$$

and  $s = f - 1$  or  $s = f - 2$ . After introducing the formula (3.2) into Eq. (3.1) the following notation has been received

$$\begin{aligned}
 (3.3) \quad & \frac{\Delta t(C + Gc_b\tau_q) + C\tau_q T_i^f}{(\Delta t)^2} \\
 &= \frac{\Delta t(C + Gc_b\tau_q) + 2C\tau_q - Gc_b(\Delta t)^2}{(\Delta t)^2} T_i^{f-1} \\
 &\quad - \frac{C\tau_q}{(\Delta t)^2} T_i^{f-2} + \frac{\lambda(\Delta t + \tau_T)}{\Delta t} \left[ \frac{1}{r} (T_r)_i^{f-1} + (T_{rr})_i^{f-1} + (T_{zz})_i^{f-1} \right] \\
 &\quad - \frac{\lambda\tau_T}{\Delta t} \left[ \frac{1}{r} (T_r)_i^{f-2} + (T_{rr})_i^{f-2} + (T_{zz})_i^{f-2} \right] + Gc_b T_b + Q_m + Q_{e_i}^{f-1}.
 \end{aligned}$$

In the next step of GFDM, in the domain considered  $\Omega = \Omega_1 \cup \Omega_2$  and along the boundary  $\Gamma = \Gamma_1 \cup \Gamma_2 \cup \Gamma_3$ , the cloud of points (nodes) is generated – cf. Fig. 2. For each node in the generated cloud the  $n$ -point star is assigned. The  $n$ -point star is composed by the central node  $N_i = (r_i, z_i)$  and surrounding points  $N_j = (r_j, z_j)$ . The selection of the points creating the star is very important for the accuracy of numerical computations. These problems are described by LISZKA and ORKISZ in [24]. In this paper, the adjacent nodes are located inside the circle of the radius  $R_d$  or the constant number  $n$  is assumed. Additionally, the regular density of nodes is under guard.

The function  $T(r, z, t)$  is expanded into the Taylor series taking into account the second derivatives

$$\begin{aligned}
 (3.4) \quad T(r, z, t) &= T(r_i, z_i, t) + \left[ \frac{\partial T(r, z, t)}{\partial r} \right]_i (r - r_i) \\
 &\quad + \left[ \frac{\partial T(r, z, t)}{\partial z} \right]_i (z - z_i) + \frac{1}{2} \left[ \frac{\partial^2 T(r, z, t)}{\partial r^2} \right]_i (r - r_i)^2 \\
 &\quad + \frac{1}{2} \left[ \frac{\partial^2 T(r, z, t)}{\partial z^2} \right]_i (z - z_i)^2 + \left[ \frac{\partial^2 T(r, z, t)}{\partial z \partial r} \right]_i (r - r_i)(z - z_i).
 \end{aligned}$$

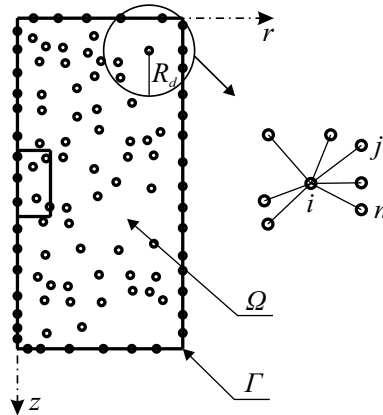


FIG. 2. Cloud of points and  $n$ -point star.

For the point  $(r_j, z_j)$  one has:

$$(3.5) \quad T_j^s = T_i^s + (T_r)_i^s h_j + (T_z)_i^s k_j \\ + \frac{1}{2}(T_{rr})_i^s h_j^2 + \frac{1}{2}(T_{zz})_i^s k_j^2 + (T_{rz})_i^s h_j k_j,$$

where  $h_j = r_j - r_i$ ,  $k_j = z_j - z_i$  and  $s$  denotes a certain time level.

The best approximation of the local values of the first and second derivatives appearing in equation (3.5) results from the least squares criterion in the form:

$$(3.6) \quad J = \sum_{j=1}^n \left\{ \left[ T_i^s - T_j^s + (T_r)_i^s h_j + (T_z)_i^s k_j \right. \right. \\ \left. \left. + \frac{1}{2}(T_{rr})_i^s h_j^2 + \frac{1}{2}(T_{zz})_i^s k_j^2 + (T_{rz})_i^s h_j k_j \right] \frac{1}{\rho_j^m} \right\}^2,$$

where

$$(3.7) \quad \rho_j = \sqrt{(r_j - r_i)^2 + (z_j - z_i)^2}.$$

In Eq. (3.6) a fraction  $1/\rho_j^m$  is the so-called weighting coefficient and usually it is assumed that  $m = 3$  [25].

In the Appendix it is shown that

$$(3.8) \quad \frac{1}{r}(T_r)_i^s + (T_{rr})_i^s + (T_{zz})_i^s = \sum_{j=1}^n Z_{ij} T_j^s - T_i^s \sum_{j=1}^n Z_{ij}.$$

Formula (3.8) is introduced into equation (3.3) and then:

$$(3.9) \quad \frac{\Delta t(C + Gc_b \tau_q) + C\tau_q T_i^f}{(\Delta t)^2} \\ = \frac{\Delta t(C + Gc_b \tau_q) + 2C\tau_q - Gc_b(\Delta t)^2}{(\Delta t)^2} T_i^{f-1} \\ - \frac{C\tau_q}{(\Delta t)^2} T_i^{f-2} + \frac{\lambda(\Delta t + \tau_T)}{\Delta t} \left( \sum_{j=1}^n Z_{ij} T_j^{f-1} - T_i^{f-1} \sum_{j=1}^n Z_{ij} \right) \\ - \frac{\lambda\tau_T}{\Delta t} \left( \sum_{j=1}^n Z_{ij} T_j^{f-2} - T_i^{f-2} \sum_{j=1}^n Z_{ij} \right) + Gc_b T_b + Q_m + Q_{e_i}^{f-1}.$$

From Eq. (3.9) the formula which allows to find the nodal temperatures results:

$$\begin{aligned}
(3.10) \quad T_i^f &= \frac{\Delta t(C + Gc_b\tau_q) + 2C\tau_q - Gc_b(\Delta t)^2}{\Delta t(C + Gc_b\tau_q) + C\tau_q} T_i^{f-1} \\
&\quad - \frac{C\tau_q}{\Delta t(C + Gc_b\tau_q) + C\tau_q} T_i^{f-2} \\
&\quad + \frac{\lambda\Delta t(\Delta t + \tau_T)}{\Delta t(C + Gc_b\tau_q) + C\tau_q} \left( \sum_{j=1}^n Z_{ij} T_j^{f-1} - T_i^{f-1} \sum_{j=1}^n Z_{ij} \right) \\
&\quad - \frac{\lambda\tau_T\Delta t}{\Delta t(C + Gc_b\tau_q) + C\tau_q} \left( \sum_{j=1}^n Z_{ij} T_j^{f-2} - T_i^{f-2} \sum_{j=1}^n Z_{ij} \right) \\
&\quad + \frac{(\Delta t)^2(Gc_bT_b + Q_m + Q_{e_i}^{f-1})}{\Delta t(C + Gc_b\tau_q) + C\tau_q}.
\end{aligned}$$

It should be pointed out that in the case of an explicit scheme application a criterion of stability should be formulated. In the case of parabolic equations a two-level difference approximation of a time derivative is used and the explicit scheme is stable, if the appropriate coefficients in the FDM are non-negative [27]. In the case of the hyperbolic equation considered here the three-level difference approximation of a time derivative is used and the problem of stability is more complicated. The equation (3.10) can be written in the form:

$$\begin{aligned}
(3.11) \quad T_i^f &= \frac{\Delta t(C + Gc_b\tau_q) + 2C\tau_q - Gc_b(\Delta t)^2 - \lambda\Delta t(\Delta t + \tau_T) \sum_{j=1}^n Z_{ij}}{\Delta t(C + Gc_b\tau_q) + C\tau_q} T_i^{f-1} \\
&\quad + \frac{\lambda\Delta t(\Delta t + \tau_T)}{\Delta t(C + Gc_b\tau_q) + C\tau_q} \sum_{j=1}^n Z_{ij} T_j^{f-1} - \frac{C\tau_q - \lambda\tau_T\Delta t \sum_{j=1}^n Z_{ij}}{\Delta t(C + Gc_b\tau_q) + C\tau_q} T_i^{f-2} \\
&\quad - \frac{\lambda\tau_T\Delta t}{\Delta t(C + Gc_b\tau_q) + C\tau_q} \sum_{j=1}^n Z_{ij} T_j^{f-2} + \frac{(\Delta t)^2(Gc_bT_b + Q_m + Q_{e_i}^{f-1})}{\Delta t(C + Gc_b\tau_q) + C\tau_q}.
\end{aligned}$$

As in the case of the two-level scheme it is assumed that the coefficients multiplied by temperatures  $T_i^{f-1}$ ,  $T_j^{f-1}$  must be non-negative. Thus

$$(3.12) \quad \frac{\Delta t(C + Gc_b\tau_q) + 2C\tau_q - Gc_b(\Delta t)^2 - \lambda\Delta t(\Delta t + \tau_T) \sum_{j=1}^n Z_{ij}}{\Delta t(C + Gc_b\tau_q) + C\tau_q} \geq 0.$$

Testing calculations have shown that this is not a sufficient criterion. An additional criterion for coefficients multiplied by temperatures  $T_i^{f-2}$ ,  $T_j^{f-2}$  has been formulated: these coefficients must be non-positive. So

$$(3.13) \quad \frac{C\tau_q - \lambda\tau_T\Delta t \sum_{j=1}^n Z_{ij}}{\Delta t(C + Gc_b\tau_q) + C\tau_q} \geq 0$$

but it is not proven mathematically.

The not very complicated problem of no-flux boundary conditions modeling is not considered here.

In Fig. 3 the algorithm of the generalized finite difference method is presented. As it can be seen, the most time-consuming operation is finding adjacent nodes, because the distances between all nodes have to be calculated. But it is important to emphasize that finding of adjacent nodes, setting and inverting  $\mathbf{G}$  matrices and calculating the  $\mathbf{Z}$  matrices is performed only once. The process of matrices inverting does not introduce a significant error because the matrices have the constant dimensions of  $5 \times 5$  and the symbolic formula is introduced.

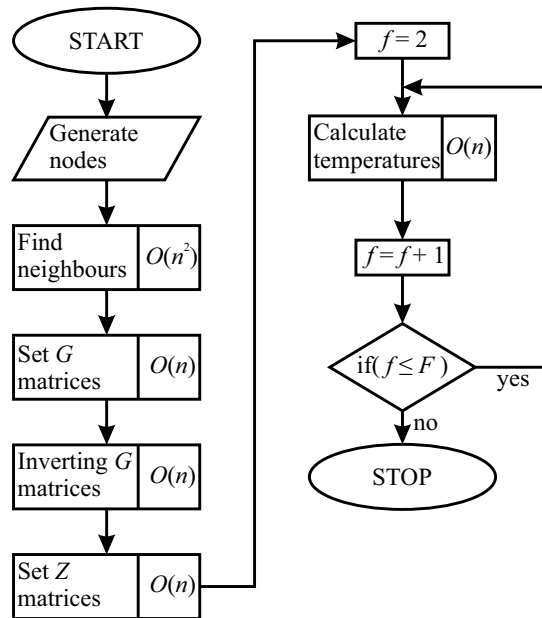


FIG. 3. Flowchart for GFDM algorithm with the order of time complexity.

To estimate an error of the generalized finite difference method, the results are compared with the results obtained using the classical finite difference method under the assumption that the grid step and time step are very small (then the FDM solution is close to the analytical one).

The absolute error is the difference between the temperatures:

$$(3.14) \quad R(T_i^f) = |(T_i^f)_{\text{FDM}} - (T_i^f)_{\text{GFDM}}|.$$

The relative error can be defined as

$$(3.15) \quad B(T_i^f) = \frac{R(T_i^f)}{|(T_i^f)_{\text{FDM}}|} = \left| \frac{(T_i^f)_{\text{FDM}} - (T_i^f)_{\text{GFDM}}}{(T_i^f)_{\text{FDM}}} \right| = \left| 1 - \frac{(T_i^f)_{\text{GFDM}}}{(T_i^f)_{\text{FDM}}} \right|.$$

Then an average relative error for each time step is calculated:

$$(3.16) \quad B_A(T^f) = \frac{1}{L} \sum_{i=1}^L \left| 1 - \frac{(T_i^f)_{\text{GFDM}}}{(T_i^f)_{\text{FDM}}} \right|,$$

where  $L$  is the number of nodes.

Finally, for  $F$  time steps the global error is equal to

$$(3.17) \quad \text{Err} = \frac{1}{F-1} \sum_{f=2}^F B_A(T^f) = \frac{1}{(F-1)L} \sum_{f=2}^F \sum_{i=1}^L \left| 1 - \frac{(T_i^f)_{\text{GFDM}}}{(T_i^f)_{\text{FDM}}} \right|.$$

#### 4. Results of computations

The cylindrical tissue domain of dimensions  $R_1 = 0.005$  m and  $Z_1 = 0.01$  m with centrally located heating zone:  $R_2 = 0.001$  m,  $Z_2 = 0.002$  m is considered (Fig. 1). In Table 1 the values of thermophysical parameters used in numerical computations are collected. As it was mentioned, the heating process takes place only inside domain  $\Omega_2$  (the exposure time  $t_{ex} = 75$  s, the power density  $Q_0 = 6$  MW/m<sup>3</sup>). On the surface of cylinder the no-flux boundary condition is assumed. The initial temperature is equal to  $T_p = 37^\circ\text{C}$ , the initial heating rate equals  $w = 0$  (cf. Eq. (2.4)). The time step is equal to  $\Delta t = 0.001$  s.

**Table 1. Thermophysical parameters [2, 5].**

Parameter	Value
Volumetric specific heat of tissue [J/(m <sup>3</sup> · K)]	$4 \cdot 10^6$
Thermal conductivity of tissue [W/(m · K)]	0.5
Specific heat of blood [J/(kg · K)]	3770
Blood perfusion rate [kg/(m <sup>3</sup> · s)]	0.53
Blood temperature [°C]	37
Metabolic heat source [W/m <sup>3</sup> ]	250
Relaxation time [s]	15
Thermalization time [s]	10

The boundary  $\Gamma$  was divided into sections with the length  $d$ . Also the interior  $\Omega$  was divided into squares (in reality, rings) having sides  $d$ . Then, on each boundary section and inside each inner square, one node has been randomly generated as shown in Fig. 4, while in Fig. 5 the all generated nodes can be seen. Two different variants of length  $d$  have been considered:  $d_1 = 0.0001$  m and  $d_2 = 0.00005$  m.

The radius  $R_d$  (cf. Fig. 2) used at the stage of selection of nodes for  $n$ -point star has been assumed as  $R_d = 5d$  or  $R_d = 10d$  ( $d = d_1$  or  $d = d_2$ ). It should be

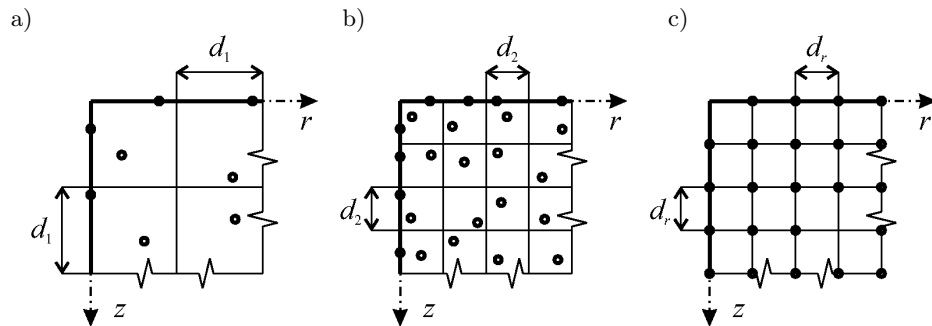


FIG. 4. Examples of nodes distribution: a)  $d_1 = 0.0001$  m, b)  $d_2 = 0.00005$  m, c) regular grid (FDM).

noted that using such a criterion of stars creation, the number of nodes used in stars is not constant. The results are presented for two points:  $N_1 = (0.005, 0.0)$  and  $N_2 = (0.005, 0.0025)$ .

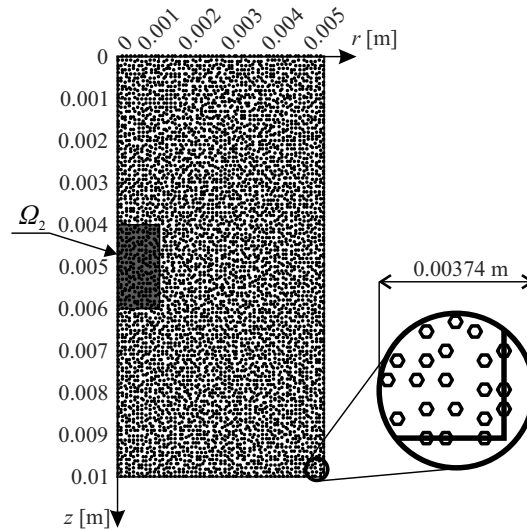
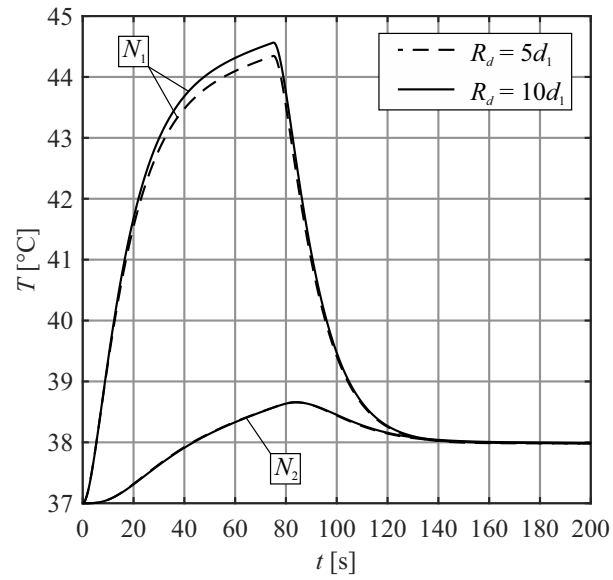
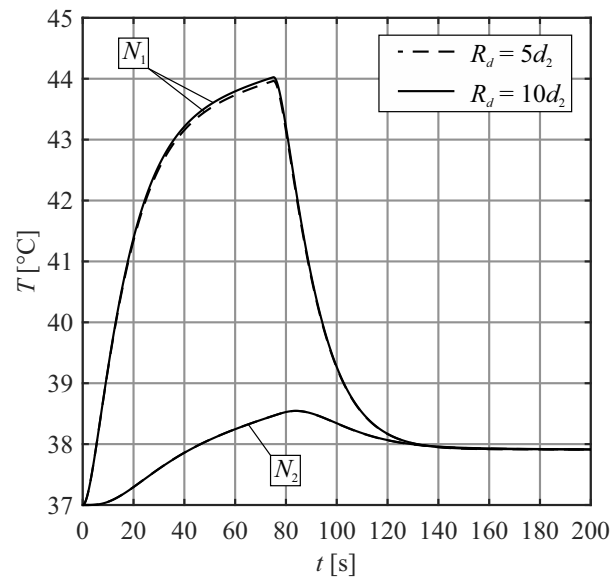


FIG. 5. An example of nodes generated inside the considered domain.

Figures 6, 7 and 8 show the temperature history at the nodes  $N_1$  and  $N_2$ . It can be seen (Fig. 6) that at the node where the heating is most intensive ( $N_1$ ), the differences between the temporary temperatures for stars corresponding to  $R_d = 5h_1$  and  $R_d = 10h_1$  are clearly visible. For the node  $N_2$ , outside the heating zone, differences are negligible.

Figure 7 illustrates that for the assumed density of nodes ( $d_1$  and  $d_2$ ) temporary temperatures at the both points are almost the same.

FIG. 6. Temperature history for density  $d_1$ .FIG. 7. Temperature history for density  $d_2$ .

In Fig. 8 the results concerning the same size of  $n$ -point star ( $R_d = 5h$ ) are shown and one can observe that the node density is important even at the point with the smaller heating intensity ( $N_2$ ).

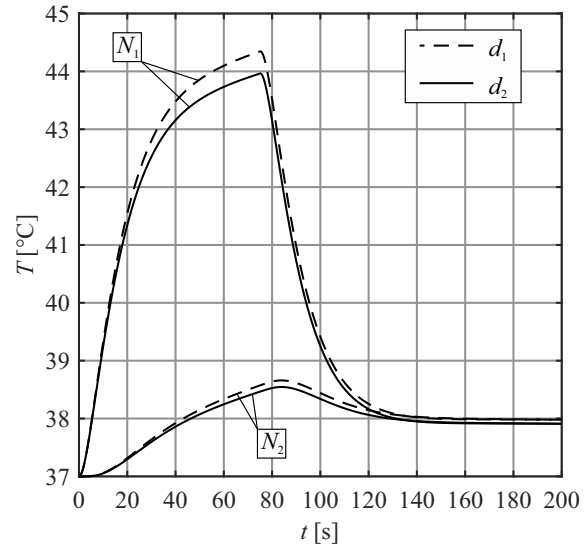


FIG. 8. Temperature history for  $R_d = 5h$ .

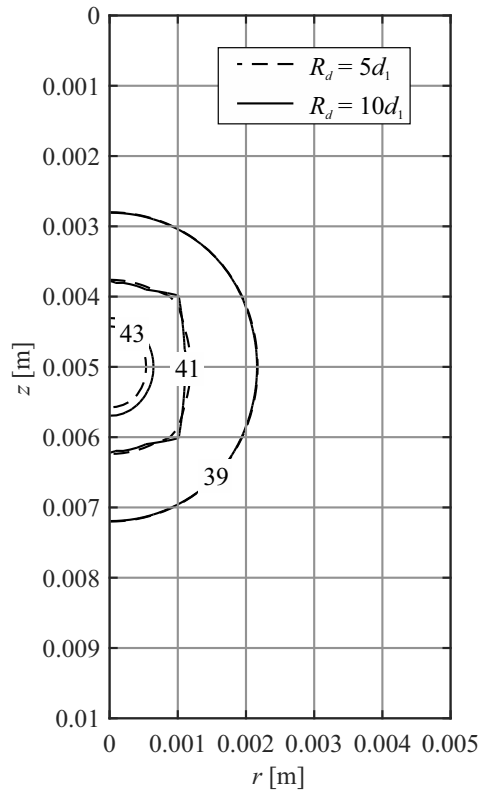


FIG. 9. Temperature distribution after 80 s for density  $d_1$ .

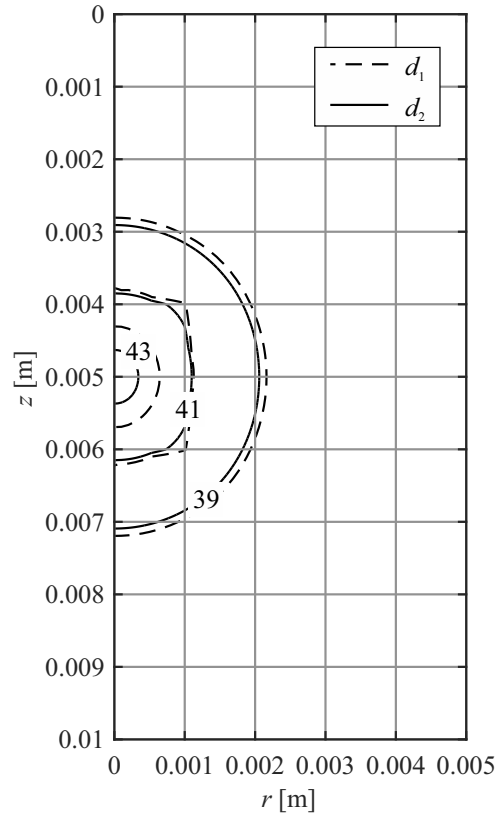


FIG. 10. Temperature distribution after 80 s for  $R_d = 10h$ .

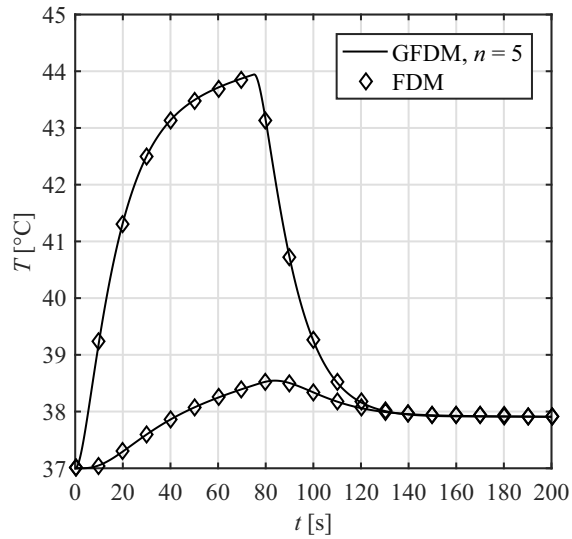


FIG. 11. Temperature history for GFDM ( $n = 5$ ) and FDM.

The temperature distribution after the time  $t = 80$  s is presented in Figs. 9 and 10. Figure 9 confirms that the differences of temperatures obtained for  $R_d = 5h_1$  and  $R_d = 10h_1$  take place only close to the heating zone.

In turn, Fig. 10 shows that differences between the nodes density cause changes in the course of isotherms both inside and outside the heating zone.

The problem considered has also been solved using the FDM algorithm for the regular spatial discretization described in [29]. In this case 5-points stars are defined (Fig. 4c), while the mesh step is equal to  $d_r = 0.00005$  m. In Fig. 11 the comparison between GFDM and FDM is shown. The results are practically the same.

The classical FDM task has also been solved using the time step  $\Delta t = 0.00001$  s and the grid  $2000 \times 1000$  nodes (i.e.,  $h = 0.000005$  m). These results allow ones to calculate the global error (cf. Eq. (3.17)). For each example presented in this paper the global error was smaller than 1 percent ( $\text{Err} < 1\%$ ).

**Table 2. Error of computations (Eq. (3.17)).**

	$d_1 = 0.0001$ m	$d_2 = 0.00005$ m
$R_d = 5d$	0.00922	0.00894
$R_d = 10d$	0.00928	0.00911
Regular grid ( $n = 5$ )	<i>N/A</i>	0.00871

## 5. Conclusions

Heating of a cylindrical tissue domain is considered. The bioheat transfer process is described by the dual-phase lag equation supplemented by an adiabatic boundary condition and appropriate initial ones. The part of domain interior is heated by an internal heat source. The problem is solved using the explicit scheme of the generalized finite difference method. The nodes creating the GFDM stars are located inside the circles of the radius  $R_d$  or the constant number of nodes  $n$  forming stars is assumed. Additionally, the regular density of nodes is under guard.

At the stage of computations the numerous numerical experiments have been done. So, the different values of nodes density and sizes of  $n$ -point stars have been considered. The changes in the courses of heating/cooling curves and also the courses of isotherms were small, but visible (see Figs. 6–10).

The comparison with the classical finite difference method with a very fine mesh also have been done. The global error for each example was smaller than one percent.

Summing up, the use of the GFDM for numerical modeling of the problem discussed leads to the satisfactory results, while the possibility of generation of

practically optional stars seems to be a very attractive tool for the approximate solution of bioheat transfer problems. The further research in this field will be devoted to more practical aspects of the modeling of cancer ablation during radiofrequency hyperthermia using the internal electrode.

### Acknowledgements

The scientific research was funded by the National Science Center of Poland, the grant no. 2015/19/B/ST8/01101, and the Silesian University of Technology, Faculty of Mechanical Engineering, the grant no. 10/990/BK\_16/0040.

### Appendix

The necessary and sufficient condition for the existence of minimum of a norm (3.6) is that the appropriate derivatives are equal to zero:

$$(A.1) \quad \begin{cases} \sum_{j=1}^n [T_i^s - T_j^s + (T_r)_i^s h_j + (T_z)_i^s k_j + \frac{1}{2}(T_{rr})_i^s h_j^2 + \frac{1}{2}(T_{zz})_i^s k_j^2 + (T_{rz})_i^s h_j k_j] \frac{h_j}{\rho_j^m} = 0, \\ \sum_{j=1}^n [T_i^s - T_j^s + (T_r)_i^s h_j + (T_z)_i^s k_j + \frac{1}{2}(T_{rr})_i^s h_j^2 + \frac{1}{2}(T_{zz})_i^s k_j^2 + (T_{rz})_i^s h_j k_j] \frac{k_j}{\rho_j^m} = 0, \\ \sum_{j=1}^n [T_i^s - T_j^s + (T_r)_i^s h_j + (T_z)_i^s k_j + \frac{1}{2}(T_{rr})_i^s h_j^2 + \frac{1}{2}(T_{zz})_i^s k_j^2 + (T_{rz})_i^s h_j k_j] \frac{h_j^2}{2\rho_j^m} = 0, \\ \sum_{j=1}^n [T_i^s - T_j^s + (T_r)_i^s h_j + (T_z)_i^s k_j + \frac{1}{2}(T_{rr})_i^s h_j^2 + \frac{1}{2}(T_{zz})_i^s k_j^2 + (T_{rz})_i^s h_j k_j] \frac{k_j^2}{2\rho_j^m} = 0, \\ \sum_{j=1}^n [T_i^s - T_j^s + (T_r)_i^s h_j + (T_z)_i^s k_j + \frac{1}{2}(T_{rr})_i^s h_j^2 + \frac{1}{2}(T_{zz})_i^s k_j^2 + (T_{rz})_i^s h_j k_j] \frac{h_j k_j}{\rho_j^m} = 0. \end{cases}$$

Let us introduce the following matrix

$$(A.2) \quad \mathbf{A} = \begin{bmatrix} \sum_{j=1}^n \frac{h_j^2}{\rho_j^m} & \sum_{j=1}^n \frac{h_j k_j}{\rho_j^m} & \sum_{j=1}^n \frac{h_j^3}{2\rho_j^m} & \sum_{j=1}^n \frac{h_j k_j^2}{2\rho_j^m} & \sum_{j=1}^n \frac{h_j^2 k_j}{\rho_j^m} \\ \sum_{j=1}^n \frac{h_j k_j}{\rho_j^m} & \sum_{j=1}^n \frac{k_j^2}{\rho_j^m} & \sum_{j=1}^n \frac{h_j^2 k_j}{2\rho_j^m} & \sum_{j=1}^n \frac{k_j^3}{2\rho_j^m} & \sum_{j=1}^n \frac{h_j k_j^2}{\rho_j^m} \\ \sum_{j=1}^n \frac{h_j^3}{2\rho_j^m} & \sum_{j=1}^n \frac{h_j^2 k_j}{2\rho_j^m} & \sum_{j=1}^n \frac{h_j^4}{4\rho_j^m} & \sum_{j=1}^n \frac{h_j^2 k_j^2}{4\rho_j^m} & \sum_{j=1}^n \frac{h_j^3 k_j}{2\rho_j^m} \\ \sum_{j=1}^n \frac{h_j k_j^2}{2\rho_j^m} & \sum_{j=1}^n \frac{k_j^3}{2\rho_j^m} & \sum_{j=1}^n \frac{h_j^2 k_j^2}{4\rho_j^m} & \sum_{j=1}^n \frac{k_j^4}{4\rho_j^m} & \sum_{j=1}^n \frac{h_j k_j^3}{2\rho_j^m} \\ \sum_{j=1}^n \frac{h_j^2 k_j}{\rho_j^m} & \sum_{j=1}^n \frac{h_j k_j^2}{\rho_j^m} & \sum_{j=1}^n \frac{h_j^3 k_j}{2\rho_j^m} & \sum_{j=1}^n \frac{h_j k_j^3}{2\rho_j^m} & \sum_{j=1}^n \frac{h_j^2 k_j^2}{\rho_j^m} \end{bmatrix}.$$

Denoting  $\mathbf{G} = \mathbf{A}^{-1}$ , one obtains the system of equations (A.1) in a matrix form:

$$(A.3) \quad \begin{bmatrix} (T_r)_i^s \\ (T_z)_i^s \\ (T_{rr})_i^s \\ (T_{zz})_i^s \\ (T_{rz})_i^s \end{bmatrix} = \begin{bmatrix} G_{11} & G_{12} & G_{13} & G_{14} & G_{15} \\ G_{21} & G_{22} & G_{23} & G_{24} & G_{25} \\ G_{31} & G_{32} & G_{33} & G_{34} & G_{35} \\ G_{41} & G_{42} & G_{43} & G_{44} & G_{45} \\ G_{51} & G_{52} & G_{53} & G_{54} & G_{55} \end{bmatrix} \begin{bmatrix} \sum_{j=1}^n \frac{h_j}{\rho_j^m} (T_j^s - T_i^s) \\ \sum_{j=1}^n \frac{k_j}{\rho_j^m} (T_j^s - T_i^s) \\ \sum_{j=1}^n \frac{h_j^2}{2\rho_j^m} (T_j^s - T_i^s) \\ \sum_{j=1}^n \frac{k_j^2}{2\rho_j^m} (T_j^s - T_i^s) \\ \sum_{j=1}^n \frac{h_j k_j}{\rho_j^m} (T_j^s - T_i^s) \end{bmatrix}.$$

Equation (A.3) allows one to determine the approximations of geometrical derivatives:

$$(A.4) \quad \begin{aligned} (T_r)_i^s &= \sum_{j=1}^n \frac{1}{\rho_j^m} (G_{11}h_j + G_{12}k_j + G_{13}h_j^2 + G_{14}k_j^2 + G_{15}h_jk_j)(T_j^s - T_i^s), \\ (T_z)_i^s &= \sum_{j=1}^n \frac{1}{\rho_j^m} (G_{21}h_j + G_{22}k_j + G_{23}h_j^2 + G_{24}k_j^2 + G_{25}h_jk_j)(T_j^s - T_i^s), \\ (T_{rr})_i^s &= \sum_{j=1}^n \frac{1}{2\rho_j^m} (G_{31}h_j + G_{32}k_j + G_{33}h_j^2 + G_{34}k_j^2 + G_{35}h_jk_j)(T_j^s - T_i^s), \\ (T_{zz})_i^s &= \sum_{j=1}^n \frac{1}{2\rho_j^m} (G_{41}h_j + G_{42}k_j + G_{43}h_j^2 + G_{44}k_j^2 + G_{45}h_jk_j)(T_j^s - T_i^s), \\ (T_{rz})_i^s &= \sum_{j=1}^n \frac{1}{\rho_j^m} (G_{51}h_j + G_{52}k_j + G_{53}h_j^2 + G_{54}k_j^2 + G_{55}h_jk_j)(T_j^s - T_i^s). \end{aligned}$$

From the system of equations (A.4) results that:

$$(A.5) \quad \begin{aligned} &\frac{1}{r} (T_r)_i^s + (T_{rr})_i^s + (T_{zz})_i^s \\ &= \frac{1}{r_i} \sum_{j=1}^n \frac{1}{\rho_j^m} (G_{11}h_j + G_{12}k_j + G_{13}h_j^2 + G_{14}k_j^2 + G_{15}h_jk_j)(T_j^s - T_i^s) \\ &\quad + \sum_{j=1}^n \frac{1}{2\rho_j^m} (G_{31}h_j + G_{32}k_j + G_{33}h_j^2 + G_{34}k_j^2 + G_{35}h_jk_j)(T_j^s - T_i^s) \\ &\quad + \sum_{j=1}^n \frac{1}{2\rho_j^m} (G_{41}h_j + G_{42}k_j + G_{43}h_j^2 + G_{44}k_j^2 + G_{45}h_jk_j)(T_j^s - T_i^s). \end{aligned}$$

After some mathematical manipulations the formula (A.5) can be written as follows:

$$(A.6) \quad \frac{1}{r}(T_r)_i^s + (T_{rr})_i^s + (T_{zz})_i^s \\ = \sum_{j=1}^n \frac{1}{\rho_j^m} \left[ \left( \frac{G_{11}}{r_i} + \frac{G_{31}}{2} + \frac{G_{41}}{2} \right) h_j + \left( \frac{G_{12}}{r_i} + \frac{G_{32}}{2} + \frac{G_{42}}{2} \right) k_j \right. \\ \left. + \left( \frac{G_{13}}{r_i} + \frac{G_{33}}{2} + \frac{G_{43}}{2} \right) h_j^2 + \left( \frac{G_{14}}{r_i} + \frac{G_{34}}{2} + \frac{G_{44}}{2} \right) k_j^2 \right. \\ \left. + \left( \frac{G_{15}}{r_i} + \frac{G_{35}}{2} + \frac{G_{45}}{2} \right) h_j k_j \right] (T_j^s - T_i^s)$$

or

$$(A.7) \quad \frac{1}{r}(T_r)_i^s + (T_{rr})_i^s + (T_{zz})_i^s = \sum_{j=1}^n Z_{ij}(T_j^s - T_i^s) = \sum_{j=1}^n Z_{ij}T_j^s - T_i^s \sum_{j=1}^n Z_{ij},$$

where

$$(A.8) \quad Z_{ij} = \frac{1}{\rho_j^m} \left[ \left( \frac{G_{11}}{r_i} + \frac{G_{31}}{2} + \frac{G_{41}}{2} \right) h_j + \left( \frac{G_{12}}{r_i} + \frac{G_{32}}{2} + \frac{G_{42}}{2} \right) k_j \right. \\ \left. + \left( \frac{G_{13}}{r_i} + \frac{G_{33}}{2} + \frac{G_{43}}{2} \right) h_j^2 + \left( \frac{G_{14}}{r_i} + \frac{G_{34}}{2} + \frac{G_{44}}{2} \right) k_j^2 + \left( \frac{G_{15}}{r_i} + \frac{G_{35}}{2} + \frac{G_{45}}{2} \right) h_j k_j \right].$$

## References

1. H.H. PENNES, *Analysis of tissue and arterial blood temperatures in the resting human forearm*, Journal of Applied Physiology, **1**, 2, 93–122, 1948.
2. M. STAŃCZYK, J. TELEGA, *Modelling of heat transfer in biomechanics, a review. Part 1. Soft tissues*, Acta of Bioengineering and Biomechanics, **1**, 4, 31–61, 2002.
3. K.N. RAI, S.K. RAI, *Heat transfer inside the tissues with a supplying vessel for the case when metabolic heat generation and blood perfusion are temperature dependent*, Heat and Mass Transfer, **35**, 4, 345–350, 1999.
4. M.C. CATTANEO, *A form of heat conduction equation which eliminates the paradox of instantaneous propagation*, Comptes Rendus, **247**, 431–433, 1958.
5. W. ROETZEL, N. PUTRA, N. NANDY, S.K. DAS, *Experiment and analysis for non-Fourier conduction in materials with non-homogeneous inner structure*, International Journal of Thermal Sciences, **42**, 6, 541–552, 2003.
6. K. MITRA, S. KUMAR, A. VEDEVARZ, M.K. MOALLEMI, *Experimental evidence of hyperbolic heat conduction in processed meat*, Journal of Heat Transfer, **117**, 3, 568–573, 1995.

7. M.N. ÖZİŞİK, D.Y. TZOU, *On the wave theory in heat conduction*, Journal of Heat Transfer, **116**, 3, 526–535, 1994.
8. K.C. LIU, Y.N. WANG, Y.S. CHEN, *Investigation on the bio-heat transfer with the dual-phase-lag effect*, International Journal of Thermal Sciences, **58**, 29–35, 2012.
9. K.C. LIU, *Thermal propagation analysis for living tissue with surface heating*, International Journal of Thermal Sciences, **47**, 5, 507–513, 2008.
10. K.C. LIU, H.T. CHEN, *Analysis for the dual-phase-lag bio-heat transfer during magnetic hyperthermia treatment*, International Journal of Heat and Mass Transfer, **52**, 5–6, 1185–1192, 2009.
11. P. KUMAR, D. KUMAR, K.N. RAI, *A numerical study on dual-phase-lag model of bio-heat transfer during hyperthermia treatment*, Journal of Thermal Biology, **49–50**, 98–105, 2015.
12. J. ZHOU, J.K. CHEN, Y. ZHANG, *Dual-phase lag effects on thermal damage to biological tissues caused by laser irradiation*, Computers in Biology and Medicine, **39**, 3, 286–293, 2009.
13. J. ZHOU, Y. ZHANG, J.K. CHEN, *An axisymmetric dual-phase-lag bioheat model for laser heating of living tissues*, International Journal of Thermal Sciences, **48**, 8, 1477–1485, 2009.
14. M.A. CASTRO, J.A. MARTIN, F. RODRIGUEZ, *Unconditional stability of a numerical method for the dual-phase-lag equation*, Mathematical Problems in Engineering, **2017**, 5, 2017.
15. S. SINGH, S. KUMAR, *Numerical study on triple layer skin tissue freezing using dual phase lag bio-heat model*, International Journal of Thermal Sciences, **86**, 12–20, 2014.
16. E. MAJCHRZAK, L. TURCHAN, J. DZIATKIEWICZ, *Modeling of skin tissue heating using the generalized dual phase-lag equation*, Archives of Mechanics, **67**, 6, 417–437, 2015.
17. H. WANG, W. DAI, R. MELNIK, *A finite difference method for studying thermal deformation in a double-layered thin film exposed to ultrashort pulsed lasers*, International Journal of Thermal Sciences, **45**, 12, 1179–1196, 2006.
18. J. McDONOUGH, I. KUNADIAN, R. KUMAR, T. YANG, *An alternative discretization and solution procedure for the dual phase-lag equation*, Journal of Computational Physics, **219**, 1, 163–171, 2006.
19. E. MAJCHRZAK, B. MOCHNACKI, *Sensitivity analysis of transient temperature field in microdomains with respect to the dual-phase-lag model parameters*, International Journal for Multiscale Computational Engineering, **12**, 1, 65–77, 2014.
20. M. CIESIELSKI, B. MOCHNACKI, *Application of the control volume method using the Voronoi polygons for numerical modeling of bio-heat transfer processes*, Journal of Theoretical and Applied Mechanics, **52**, 4, 927–935, 2014.
21. E. MAJCHRZAK, *Numerical solution of dual phase lag model of bioheat transfer using the general boundary element method*, CMES: Computer Modeling in Engineering and Sciences, **69**, 1, 43–60, 2010.
22. E. MAJCHRZAK, L. TURCHAN, *The general boundary element method for 3D dual-phase lag model of bioheat transfer*, Engineering Analysis with Boundary Elements, **50**, 76–82, 2015.

- 
23. B. YU, W.A. YAO, H.L. ZHOU, H.L. CHEN, *Precise time-domain expanding BEM for solving non-Fourier heat conduction problems*, Numerical Heat Transfer, Part B: Fundamentals, **68**, 6, 511–532, 2015.
  24. T. LISZKA, J. ORKISZ, *The finite difference method at arbitrary irregular grids and its application in applied mechanics*, Computers and Structures, **11**, 1–2, 83–95, 1980.
  25. L. GAVETE, J.J. BENITO, F. UREÑA, *Generalized finite differences for solving 3D elliptic and parabolic equations*, Applied Mathematical Modelling, **40**, 2, 955–965, 2016.
  26. L. GAVETE, F. UREÑA, J.J. BENITO, A. GARCÍA, M. UREÑA, E. SALETE, *Solving second order non-linear elliptic partial differential equations using generalized finite difference method*, Journal of Computational and Applied Mathematics, **318**, 378–387, 2017.
  27. B. MOCHNACKI, E. PAWLAK, *Numerical modelling of non-steady thermal diffusion on the basis of generalized FDM*, [in:] Advanced Computational Methods in Heat Transfer V, Computational Studies, 33–42, 1998.
  28. B. MOCHNACKI, E. MAJCHRZAK, *Numerical modeling of casting solidification using generalized finite difference method*, [in:] THERMEC 2009, Materials Science Forum, **638**, 2676–2681, Trans Tech Publications, 2010.
  29. E. MAJCHRZAK, L. TURCHAN, G. KALUŻA, *Sensitivity analysis of temperature field in the heated tissue with respect to the dual-phase-lag model parameters*, [in:] Advances in Mechanics: Theoretical, Computational and Interdisciplinary Issues, M. Kleiber, T. Burczyński, K. Wilde, J. Górski, K. Winkelmann, L. Smakosz (Eds.), CRC Press/Balkema, 371–375, 2016.

Received December 5, 2016; revised version April 5, 2017.

---